since 1961

Baltica

BALTICA Volume 37 Number 1 June 2024: 24–38
https://doi.org/10.5200/baltica.2024.1.3

Determination of the shear wave velocity structure of substations by the HVSR inversion method using broadband and strong ground motion earthquake data in the Lake Van region, eastern Türkiye

İsmail Akkaya*, Hamdi Alkan

Akkaya, İ., Alkan, H. 2024. Determination of the shear wave velocity structure of substations by the HVSR inversion method using broadband and strong ground motion earthquake data in the Lake Van region, eastern Türkiye. *Baltica, 37* (*1*), 24–38. Vilnius. ISSN 0067-3064.

Manuscript submitted 30 October 2023 / Accepted 15 April 2024 / Available online 23 May 2024

Abstract. In this research, the horizontal-to-vertical spectral ratio analysis and the Monte-Carlo inversion algorithm are applied to calculate the substations shear wave velocity structure beneath the Lake Van region. To discover the variation of shear wave velocity, the local earthquakes recorded on 15 strong ground motions and 14 broadband stations, located on dissimilar geological units, are used. The most important aim of this investigation is to reveal the geological structure and bedrock depths beneath each station. For this purpose, two-dimensional cross-sections are generated from velocity models in different directions. The average bedrock depth variation is determined at 10 m and 250 m as a result of the horizontal-to-vertical spectral ratio inversions at the earthquake stations in the region. The deepest bedrock depths are calculated at the earthquake stations close to the settlements in the study area. These depth variations are interpreted as the local site effects of possible destructive and big earthquakes that may be a factor increasing the damage ratio in these regions.

Keywords: *spectral ratio; Vs velocity analysis; bedrock depth*

Akkaya İsmail (iakkaya@yyu.edu.tr) https://orcid.org/0000-0002-7682-962X*
Hamdi Alkan (hamdialkan@yyu.edu.tr), https://orcid.org/0000-0003-3912-7503
Van Yüzüncü Yıl University, Department of Geophysical Engineering, Van, Türkiye
**Corresponding author*

INTRODUCTION

The occurrence of earthquake effects on the ground surface and structural elements corresponds to the combination of site characteristics, source, and path. In addition to the magnitude of the earthquake, site conditions play a critical role in the earthquakes effect on infrastructure. Near-surface soils, which may be stable under static conditions, can cause ground failure under the effect of a dynamic force, such as an earthquake, by influencing the properties of the soil layers through which they pass in various ways (soil amplification, liquefaction, etc.). Furthermore, an earthquake that appears to have no effect above stiff soil can be felt like a strong motion and cause severe damage in specific areas above soft sediments due to the amplification of seismic waves. Understanding the behaviour of soils under static loading and determining the behaviour of soils under dynamic loading, like earthquakes, can lead to significant reductions in structural damage.

Estimating shear wave velocity (Vs) and thickness in a geological structure composed of soft and unconsolidated alluvial units is extremely important for measuring the local site effect caused by a destructive earthquake. Also, the determination of shear wave velocities is a starting parameter for soil response analysis and engineering applications. Vs is one of the most significant engineering design parameters in soil modelling, particularly in the sediment

layer above the bedrock. Seismic bedrock depth, which must be determined in terms of engineering seismology, seismic risk analysis, acceleration, and evaluation of earthquake effects, is defined by shear wave velocities. Many shallow and deep investigation methods such as seismic refraction, MASW, ReMi, seismic reflection, and SPAC can be used to calculate Vs velocity variation. In addition to these, Vs variation can be generated by the horizontal-to-vertical spectral ratio (HVSR) curve inversion process. The HVSR curve inversion is sensitive to velocity contrasts and has numerous advantages, including relatively fast data processing time and low survey costs. In recent years, the use of HVSR techniques for subsurface investigations has increased (Herak 2008; Bignardi *et al*. 2016).

There are many valuable studies in the literature related to the HVSR algorithm which is a widespread tool used to map resonance frequencies in engineering seismology exploration for constraining shallow geological structures (Nakamura 1989, 2000; Fah *et al*. 2001; Lermo, Chavez-Garcia 1994; Lachet, Bard 1994). This previous research indicates that when there is a major impedance contrast between the sediments and the bedrock, the HVSR highest value can be used to forecast the predominant resonance frequency of the associated region. By correlating the measured soil resonance frequencies with the thickness of the resonance layer, the bedrock depth can be determined. The first stratigraphic application of the HVSR procedure was proposed by Ibs-von Seht and Wohlenberg (1999). On the other hand, in many previous studies, the relationship between the bedrock depth and the predominant frequency has been carried out (Parolai *et al*. 2002; Tün *et al*. 2016; Büyüksaraç *et al*. 2022, 2023). Lermo and Chavez-Garcia (1993) demonstrated that the HVSR method can be applied to shear waves, which are the strongest section of earthquake data records. Since then, many studies have been carried out to determine the applicability and restrictions of the HVSR for both ambient noise and earthquakes (Lachet, Bard 1994; Parolai *et al*. 2002).

This study aims to investigate substation geological structure and bedrock depths at shear wave velocities obtained by using the HVSR analysis of broadband and strong-motion earthquake data. Therefore, the earthquake horizontal-to-vertical spectral ratio (EHVSR) process is used to analyse twenty-two earthquake records from local earthquakes in the Lake Van area recorded by twenty-nine (15 strong-motion, 14 broadband) stations located in different geological formations.

The EHVSR method, proposed by Langston (1977), suppose that the vertical motions are unaffected by local soil conditions and horizontal motions are influenced by underground layers. The method of Langston (1977) was used to determine the geological structure of the crust and mantle from teleseismic earthquake. It has been stated by different researchers that EHVSR analysis can be used to identify the possible structural damage caused by devastating and destructive earthquakes without a reference measurement station (Lachet *et al*. 1996; Bard 1998; Lermo, Chavez Garcia 1993, 1994; Nakamura 2000, 2008; Akkaya, Özvan 2019; Pamuk 2019; Pamuk, Özer 2020; Gupta *et al*. 2021; Aydın *et al*. 2022; Akkaya 2023). In addition, according to Langston (1977), this algorithm provides information on local site effects that are independent of the properties of the path and the source.

In this study, substation velocity structure, bedrock depth and soil characteristics in the Lake Van area surrounded by the broadband and accelerometer stations (Table 1) are calculated using the earthquake records greater than the magnitude of 4.5 that occurred between 2011–2021 (Table 2). The earthquake records were collected at the accelerometers managed by the Disaster and Emergency Management Authority of Türkiye (AFAD). The broadband earthquake records were provided by the AFAD and the Kandilli Observatory and Earthquake Research Institute (KOERI) stations (Table 1). At each station, the predominant periods of the soil and the EHVSR amplitude value were determined. Substation Vs velocity changes with depth-dependent and bedrock depths were also calculated using one-dimensional inversion models. The tectonic structure, seismicity, and engineering properties of the region are evaluated with the 2-D cross-sections created by the velocity models.

REGIONAL GEOLOGY AND TECTONICS

The Lake Van region is composed of various kind of rock units and alluvial units. The region is made up of three widespread geological units: Palaeozoic metamorphic rocks and the Upper Cretaceous ophiolites, the volcanic rocks, and the Miocene and Quaternary alluvium. The most common geological units on the eastern side of the Lake Van basin are alluvial deposits and lake sediments. The Lake Van basin was formed by the evolution of continental collision between the Arabian and Eurasian mega plates and affected the regional tectonic activity. The region was formed as a result of the thickening, shortening, and uplift of the East Anatolian crust (Şengör, Kidd 1979; Şaroğlu, Yılmaz 1986; Koçyiğit *et al*. 2001) due to the influence of the continental collision that started in the Late Miocene (Fig. 1). The final shape of the region with the volcanism was effective in the Quaternary period. The north-south directional compressional tectonic properties in the Eastern Anatolian

Table 1 Information on broadband and strong motion stations used in the study

Station Code	Name	Station Location	Longitude	Latitude	Elevation	Number of records
6501	Afad_SM	Van	43.401	38.503	1745	13
6503	Afad_SM	Muradiye	43.763	38.990	1712	9
6505	Afad_SM	Çaldıran	43.901	39.135	2043	6
6506	Afad_SM	Erciş	43.337	39.019	1681	6
6507	Afad_SM	Gevaş	43.119	38.296	1696	7
6508	Afad_SM	Özalp	43.976	38.657	1994	8
6510	Afad_SM	Edremit	43.268	38.414	1850	7
6512	Afad_SM	Muradiye	43.762	38.989	1712	2
6513	Afad_SM	Edremit	43.268	38.414	1850	4
6514	Afad_SM	Gürpınar	43.408	38.322	1787	4
1302	Afad_SM	Bitlis	42.159	38.474	1794	13
1303	Afad_SM	Adilcevaz	42.763	38.799	1678	3
1304	Afad_SM	Tatvan	42.280	38.503	1676	4
1305	Afad_SM	Güroymak	42.021	38.580	1307	4
1306	Afad_SM	Ahlat	42.489	38.755	1715	4
VANB	KOERI_BB	Van	43.405	38.509	1627	11
AKDM	KOERI_BB	Akdamar	42.980	38.328	1662	6
CLDR	KOERI_BB	Çaldıran	43.917	39.144	2094	10
ERCV	KOERI_BB	Erciş	43.338	39.019	1697	10
GURO	KOERI_BB	Güroymak	42.032	38.550	1388	6
MLAZ	KOERI_BB	Malzagirt	42.549	39.141	1581	5
AGRB	KOERI_BB	Ağrı	42.992	39.575	1820	13
VRTB	KOERI_BB	Varto	41.455	39.160	1498	10
BLIS	AFAD_BB	Bitlis	42.115	38.414	1608	3
GEVA	AFAD_BB	Gevaş	43.058	38.312	1672	14
ADCV	AFAD_BB	Adilcevaz	42.724	38.808	1774	8
TVAN	AFAD_BB	Van	43.404	38.523	1970	9
VMUR	AFAD_BB	Muradiye	43.571	38.989	1717	12
OZAP	AFAD_BB	Özalp	43.992	38.661	2058	3

region controls to the northwest and northeast trending strike-slip faults, east-west trending thrusts faults, and north-south trending normal faults (Koçyiğit *et al*. 2001; Koçyiğit 2013; Toker *et al*. 2017a, b; Sengul *et al*. 2019; Özer *et al*. 2022; Alkan *et al*. 2023). In addition, north-south oriented opening cracks control the eruption centres of volcanoes and east-west axis folds developed perpendicular to this compression (Şaroğlu, Yılmaz 1986). Strike-slip and thrust characteristics faults are the dominant tectonic forms such as the Van, Özalp, Alaköy, and Yeniköşk thrust fault, Çaldıran, Erciş-Kocapınar, Başkale, Çolpan, and Gürpınar strike-slip fault zone (Koçyiğit 2013; Utkucu 2013; Akkaya 2015, 2020a, b; Akkaya *et al*. 2015; Sengul *et al*. 2019; Akkaya, Özvan 2019; Alkan, Akkaya 2023). Due to the tectonic movement in the Lake Van region, numerous destructive earthquakes have occurred in both instrumental and historical periods (Fig. 1). The most important ones are the 1976 Çaldıran earthquake (M_s = 7.3), 2011 Van earthquake (M_w = 7.1), 2020 Khoy-Başkale earthquake (M_w = 5.9), and the Saray earthquake (M_w = 5.4) in 2020 (Özvan *et al*. 2005; Tan *et al*. 2008; Akkaya 2015; Akkaya *et al*. 2018; Sengul *et al*. 2019; Akkaya, Özvan 2019; Alkan *et al*. 2020).

PROCESSING OF THE EARTHQUAKE DATA

During the period from October 2011 to October 2021, 22 earthquakes with magnitude 4.5 < M_w were recorded in the twenty-nine permanent seismic stations (14 broadband stations, 15 strong-motion stations) in the study region (Fig. 1 and Table 1). The earthquake records were retrieved from the AFAD and European Integrated Data Archive (EIDA), just as the ground motion records were retrieved from the AFAD. The triaxial seismogram waveforms and amplitude spectra of the earthquake (M_w = 5.4) occurred on 25 June 2020 at 10:03 pm (UTC) and in the southeast from Van city are shown in Figs 2, S1 and S2. The strong motion waveform for station 6505 is shown in Fig. 2, while the broadband waveforms for stations CLDR and TVAN are presented in Figs S1 and S2 (see details in the supplementary file). Demonstrating the efficacy of earthquake and ground motion records, the selected acceleration recordings, velocity-time histories and their Fourier amplitude spectra are compared in the time and frequency domain. The Fourier spectra of each component show the presence of low-frequency

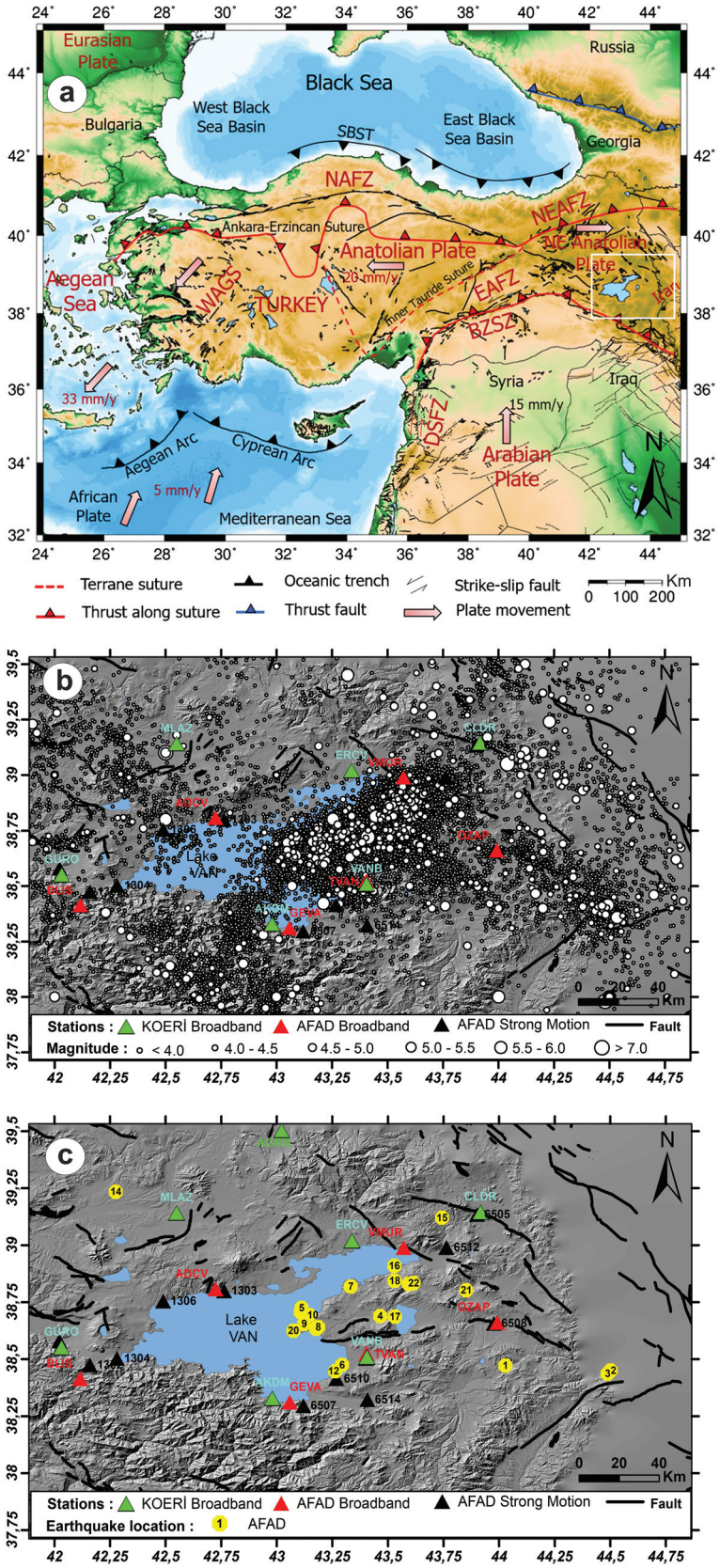

Fig. 1 (**a**) The main tectonic elements in and around Turkey (obtained from Alkan *et al*. 2021). The study region is shown in a white rectangular frame. Abbreviations: WAGS: West Anatolian Graben System; EAFZ: East Anatolian Fault Zone; NAFZ: North Anatolian Fault Zone; NEAFZ: Northeast Anatolian Fault Zone; BZSZ: Bitlis-Zagros Suture Zone; DSFZ: Dead Sea Fault Zone. (**b**) The seismicity of the study region. For the map, earthquakes with a magnitude greater than 4.0 between 1900 and 2021 are used. The catalogue information of earthquakes is taken from KOERI. The regional fault structures were modified from Emre *et al*. (2018). (**c**) AFAD and KOERI station distributions and the locations of the earthquakes for the analysis

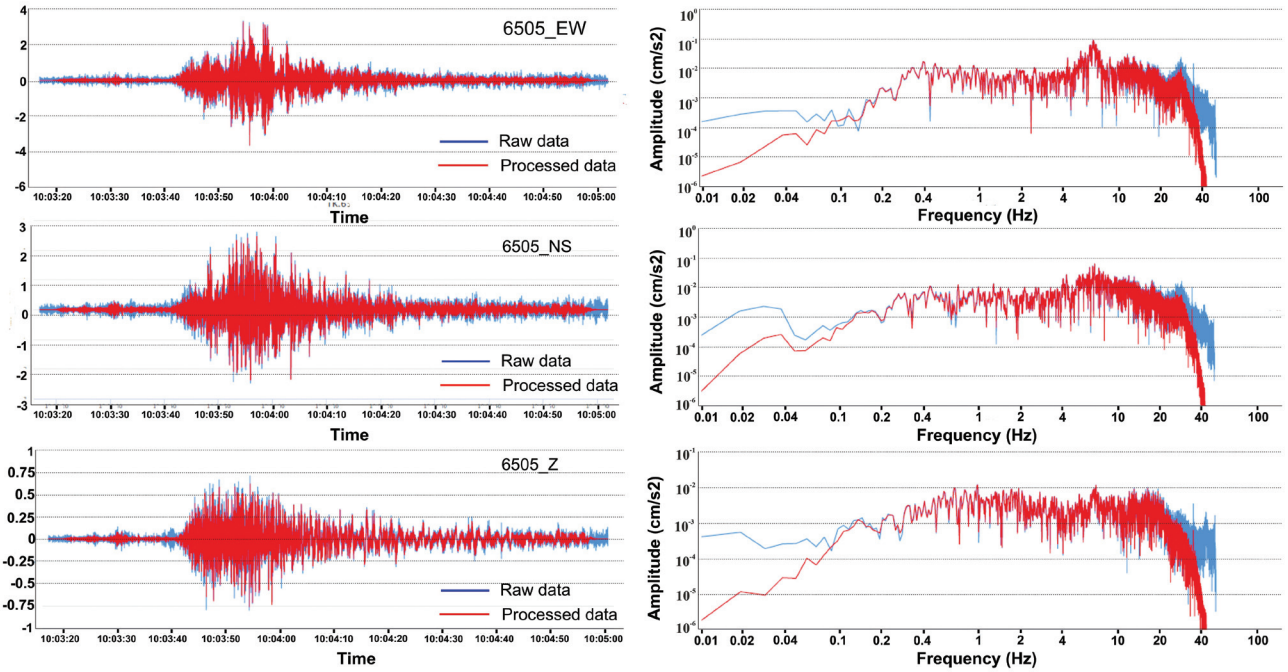

Fig. 2 An example of the triaxial seismogram waveform (E–W, N–S, and vertical) and amplitude spectra for the Van-Saray earthquake (44.02^{0}N, 38.47^{0}E, M_w = 5.4, and h = 7.48 km), which occurred on 25 June 2020 and was recorded at AFAD strong motion station 6505

waves (0.1–40 Hz) and their big amplification factor at the area (Fig. 2). In broadband station recordings, the presence and amplification of high-frequency (>10 Hz) waves can be seen (Figs S1 and S2).

When assessing the EHVSR spectra, the S-wave part of each earthquake or the whole earthquake data was manually selected to calculate the Fourier amplitude spectrum (FAS) of components (NS, EW, Z) obtained at each station. At each earthquake station site, a trend analysis was applied to data for the removing base-line correction from the raw data. For signal stabilization, the three-component waveform data were digitized at a rate of 100 samples per second (100 Hz). The window length was chosen as the duration of each earthquake to determine local soil effects. Amplitude spectrums were calculated for each select window using the Fourier transform algorithm. The recorded data were filtered using a Butterworth bandpass filter with a frequency range of 0.01–25 Hz. The spectra were smoothed using smoothing parameter 40. And then, the average spectral ratio of components was obtained to reflect the soil characteristics of the station site. And finally, the EHVSR curve with fundamental frequency (f_0) and highest amplitude values were obtained (Fig. 3, Table 2). The records have been processed using GEOPSY software.

The average EHVSR curves for each station data are displayed in Figs 3, S3 and S4. For the EHVSR curves, the shear-wave windows were taken from the seismograms with the shear-wave signals of maximum time duration. The analysed data demonstrated three shapes of HVSR result curves with low, broad, and clear amplitude HVSR peaks. The HVSR shape is relevant to the impedance contrast, with a sharp peak indicating a high impedance contrast between the overlying soft sediments and the underlying bedrock, according to Bonnefoy-Claudet *et al*. (2009). In the observed records for each station, amplitudes were generally obtained between 0.5 and 5.0 Hz, except for 6505, TVAN, and ADCV (Figs 3 and S4). Most of the stations (6501, 6503, 6506, 6507, 6508, 6512, 6514, 1303, 1304, VANB, GURO, VRTB, ERCV, and OZAP) are located on alluvial type of geological units known to have weak engineering properties, whereas stations 6505, 1302, 6513, CLDR, BLIS, ADCV, TVAN, VMUR, and GEVA are deployed on the stiff soil and rock. A high-frequency amplitude (> 5 Hz) was measured in this station, indicating a thin soft-weak sediment layer laying over the rocks. The curves of 1306 and AKDM showed a flat curve with low amplitude spectra without a described curve peak (Figs 3 and S3). Multiple HVSR peaks (6505, 6507, 6510, 1302, 1303, VANB, AGRB, TVAN, OZAP, and BLIS) were often observed in areas where the local lateral variations due to complex subsurface formations cause peak broadening (Figs 3, S3, and S4, see details in the supplementary file).

EHVSR INVERSION

Geophysical inversion is a method that can be

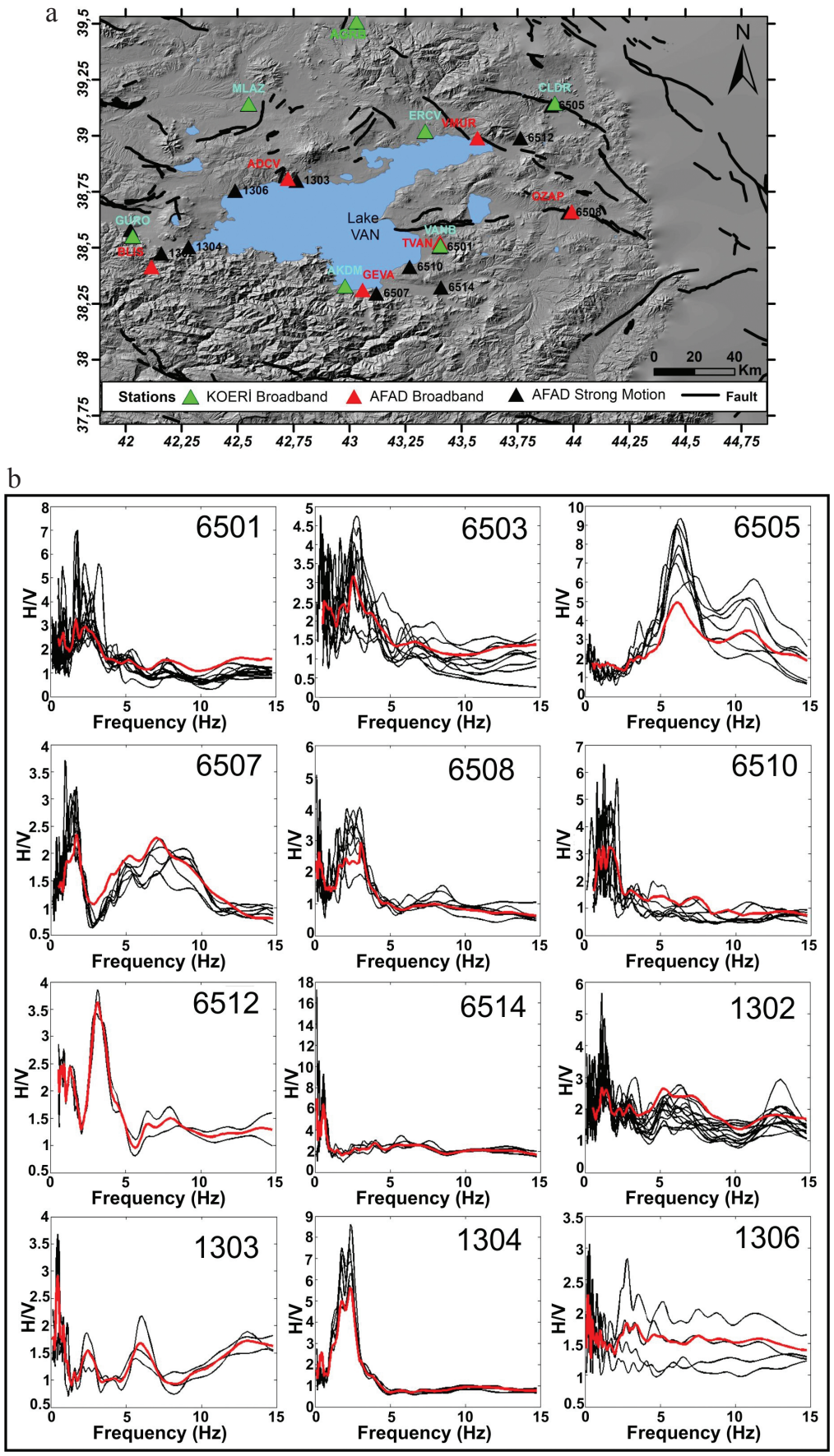

Fig. 3 (**a**) The map shows the locations of the broadband and strong motion stations. (**b**) The information on the fundamental resonance frequency and amplitude values of the AFAD strong motion stations. Each black curve represents a different earthquake record curve for each station, and the red thick lines show the average EHVSR curves

Table 2 Locations and parameters of selected earthquakes and stations

No	Date	Epicenter Location		Magnitude		Depth	PGA (cm/sn2)	KOERI Broadband							AFAD Broadband						AFAD Strong motion												
		Long	Lat	Type	M			AKDM	CLDR	GURO	MLAZ	ERCV	VANB	AGRB	VRTB	TVAN	VMUR	OZAP	GEVA	BLIS	ADCV	6501	6503	*6505*	6506	6507	6508	6510	6512	6513	6514	1302	1303	1304	1305	1306
1	25.06.2020	44.028	38.472	M_w	5.4	7.48	34.12	x	x	x	x	x		x	x	x	x	x	x	x	x	x		x		x	x		x	x	x	x		x	x	x
2	23.02.2020	44.502	38.450	M_w	5.9	8.1	17.69	x		x	x					x	x	x	x	x	x	x		x	x	x	x			x	x	x	x	x	x	x
3	23.02.2020	44.489	38.436	M_w	5.9	14.9	15.057	x		x	x					x	x	x	x	x	x	x		x	x	x	x			x	x	x	x	x	x	x
4	23.10.2011	43.465	38.689	M_w	7	19.02	178.35									x	x		x				x									x				
5	14.11.2011	43.111	38.725	M_L	5.1	18.75	23.27		x			x	x	x		x	x		x		x	x	x					x				x				
6	30.11.2011	43.294	38.474	M_L	5	14.76	104.75		x							x	x		x		x	x	x		x	x	x									
7	23.10.2011	43.333	38.818	M_L	5.5	17.3	38.0							x	x	x	x		x				x									x				
8	23.10.2011	43.186	38.640	M_L	5	16.75	4.34						x	x			x		x													x				
9	23.10.2011	43.123	38.654	M_L	5.8	13.96	20.88								x				x													x				
10	24.10.2011	43.147	38.693	M_L	4.8	18.71	13.09						x	x	x				x			x										x				
11	25.10.2011	43.594	38.829	M_L	5.5	18.28	18.71										x		x			x										x				
12	09.11.2011	43.263	38.447	M_L	5.6	6.09	245.9		x			x		x			x		x		x	x	x					x				x				
13	08.11.2011	43.108	38.706	M_L	5.4	6.9	19.5		x			x	x	x		x	x		x		x	x	x					x								
14	26.03.2012	42.276	39.234	M_L	5	17.0	58.5		x	x						x	x		x		x												x			
15	29.10.2015	43.743	39.119	M_L	4.8	4.9	77.36	x	x	x	x	x	x	x	x									x	x	x	x		x							
16	03.04.2020	43.529	38.909	M_W	4.7	12.99	4.13	x		x	x	x		x	x							x			x	x	x			x	x	x		x	x	x
17	24.10.2011	43.532	38.686	M_L	4.7	18.89	6.96						x									x										x				
18	02.11.2011	43.530	38.843	M_L	4.8	21.71	5.5		x			x	x		x							x	x					x								
19	12.11.2011	43.177	38.632	M_L	4.5	18.9	3.99		x			x	x	x	x							x	x		x			x								
20	14.11.2011	43.075	38.624	M_L	4.7	18.98	2.2					x	x	x														x								
21	18.11.2011	43.852	38.802	M_L	5.2	8.0	9.26		x			x	x	x	x								x	x			x	x								
22	06.12.2011	43.616	38.833	M_L	4.7	15.36	7.41						x	x	x									x	x		x									

used to reveal the subsurface distribution of physical property from data collected in any field. In other words, the inversion is the calculation of mathematical model parameters that allow us to determine these parameters from the data. The EHVSR method does not provide the Vs velocity structure directly; however, it can be derived by the numerical modelling of the spectral ratio result curve. In the EHVSR technique, the inversion data procedure can be used to recognize the Vs velocity value by minimizing the objective function, namely the difference between calculated and observed data. Many studies have been conducted to reliably identify Vs velocity models and the inversion of EHVSR curves (Herak 2008; Sanchez-Sesma *et al*. 2011; Bignardi *et al*. 2016, 2018). Inversion plays a critical role in modelling EHVSR curves to understand the response of complex subsurface geology, particularly when the near-surface is in a multilayered sedimentary structure (Bignardi *et al*. 2016, 2018).

The ModelHVSR software (Herak 2008) is a useful software to determine the 1-D distribution of underground elastic properties by the inversion of EHVSR result curves. The OpenHVSR open-source software (Bignardi *et al*. 2018) is widely used to calculate two- and three-dimensional underground models. In this study, OpenHVSR was used for the inversion of EHVSR curve for deriving Vs of subsurface (Bignardi *et al*. 2018). The algorithm uses a guided Monte-Carlo inversion (GMCI) method, in which the Vs velocity model modified in an initial model search space depends on the misfit function between the observed and synthetic curves (Herak 2008; Bignardi *et al*. 2018). Thus, sufficient control is provided to constrain discrete sections of the curves. The error function is composed of three terms, such as the regularization term, the misfit function between the data and the synthetic, and the slope term (Bignardi *et al*. 2016).

In the inversion of the EHVSR curves, the initial models were created to investigate the values of the subsurface elastic parameters in a wide range and

Table 3 Initial model parameters used in the EHVSR inversion process

Compressional Wave Velocity, Vp (m/s)	Shear Wave Velocity, Vs (m/s)	Density ρ (kg/m^3)	Thickness h (m)	Quality factors with P-velocity Qp	Quality factors with S-velocity Qs
1730	1000	1.95	10	10	5
1730	1000	1.95	10	10	5
1730	1000	1.95	30	15	10
1730	1000	1.95	30	15	10
1730	1000	1.95	50	30	20
1730	1000	1.95	50	30	20
1730	1000	1.95	100	40	30
1730	1000	1.95	100	40	30
1730	1000	1.95	200	40	30
1730	1000	1.95	999	999	999

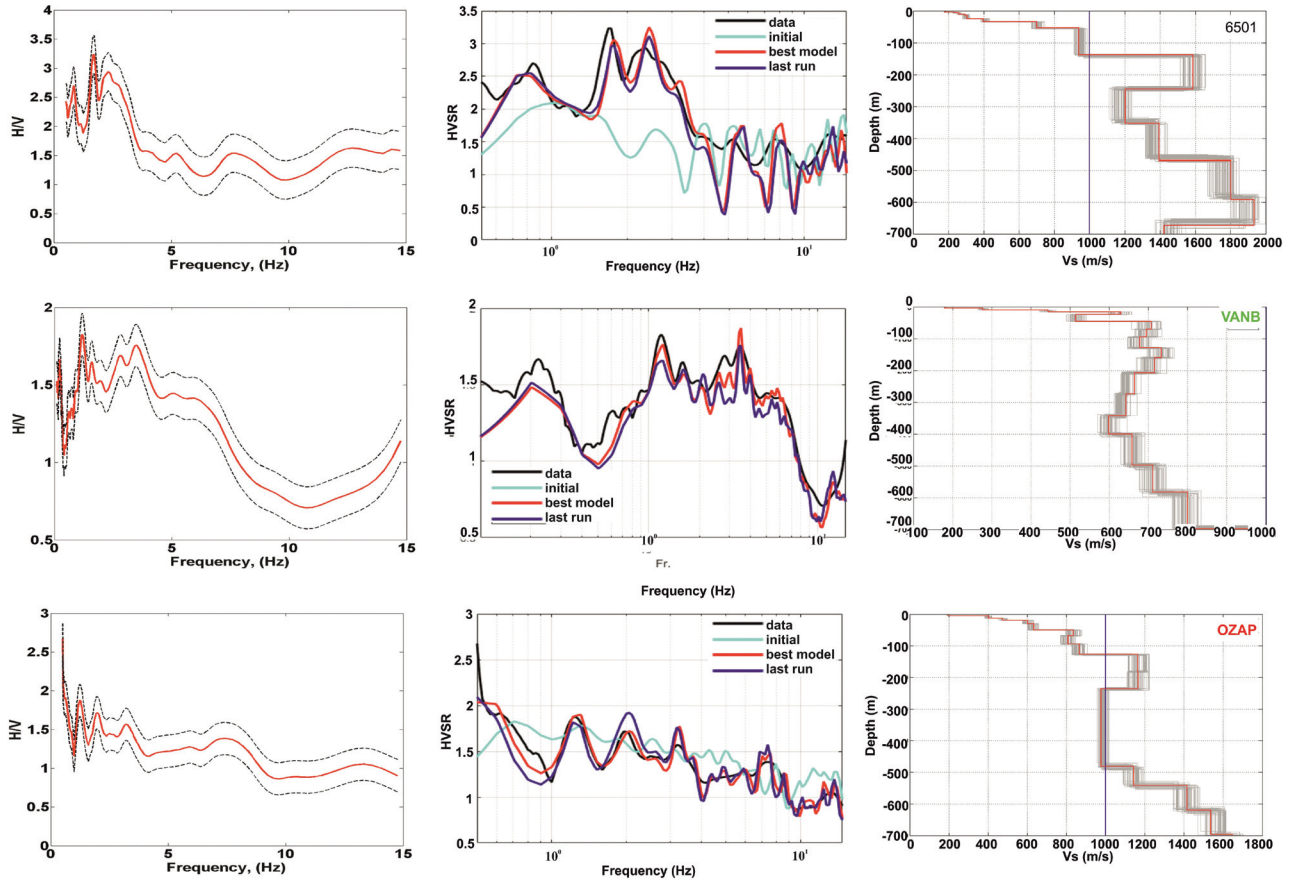

Fig. 4 The inversion results for the strong motion (6501) and broadband stations (VANB and OZAP). The left panel shows the mean curves and standard deviations, the middle panel shows the inversion results, and the right panel demonstrates the best Vs velocity models

were performed using OpenHVSR software (Bignardi *et al*. 2018). The initial models consisted of n-number of visco-elastic horizontal layers, defined by compressive wave velocity (Vp) and shear wave velocity (Vs), density (ρ), thickness (h), and the frequency-dependent corresponding attenuation factors (Qp and Qs) controlled the inelastic characteristics (Aki, Richards 2002; Bignardi *et al*. 2018).

The data inversion procedure also needs model parameters (Vp, Vs, ρ, h, Qp and Qs) as initial values (see Table 3). Due to the width of the study region and the limited number of shallow borehole (< 50 m) data, the constant parameter model was used to define the initial values (Table 3). Also, the GMCI algorithm requires several iterations and a standard deviation of random normal to initialize the model parameters (Herak 2008; Bignardi *et al*. 2018). During the inversion, the theoretical response obtained from the initial model is compared to the observed EHVSR results. After each iteration, a new minimum misfit is determined, and then the corresponding subsurface model is set as the reference. After enough investigation of

model parameters, the most suitable model can be found (equal to the previous iteration or minimum misfit) according to the assumed wave propagation. Finally, the best fitting model is achieved with many random generations ranging between 10^2 and 10^4. The last model of inversion process is a 1-D velocity model corresponding between Vs and depth. Figs 4, 5 and S5–S9 show the results of the inversion process in the earthquake station.

The EHVSR inversion results were calculated for all earthquake stations. However, the mean curves, EHVSR inversion model results, and the best Vs velocity models are presented for the eight observation points (Figs 4 and S5–S6, see details in the supplementary file). The black and red curves represent the observed mean HVSR curves and are inverted from the best fit of the Vs velocity models obtained from the GMCI results. The thin black curve lines are plotted to demonstrate standard deviations in the EHVSR curves. The cyan lines display the initial model, and the blue line represents to last run to the inversion (Figs 4 and S5–S6). Beneath each station, 1–D Vs velocity model sections are given in Figs 5 and S7–S9. The solid red lines represent the best models, while the grey lines represent the acceptable model numbers.

One broadband station (ERCV) and four acceleration stations (6501, 6505, 6508, and 6510) operated by AFAD were selected for detailed evaluation. The selected earthquake stations are located in the vicinity of densely populated areas in the region. However, borehole data and near-surface velocity data are not available for the majority of measurement stations in the area. In the available earthquake station geological site investigation, only the borehole data of station 6501, located in the settlement centre of Van, are provided (https://tadas.afad.gov.tr/list-station). The Vs velocity values and borehole logs for other selected stations were obtained from Akkaya and Özvan (2019) and Akkaya *et al*. (2018) from the data in their

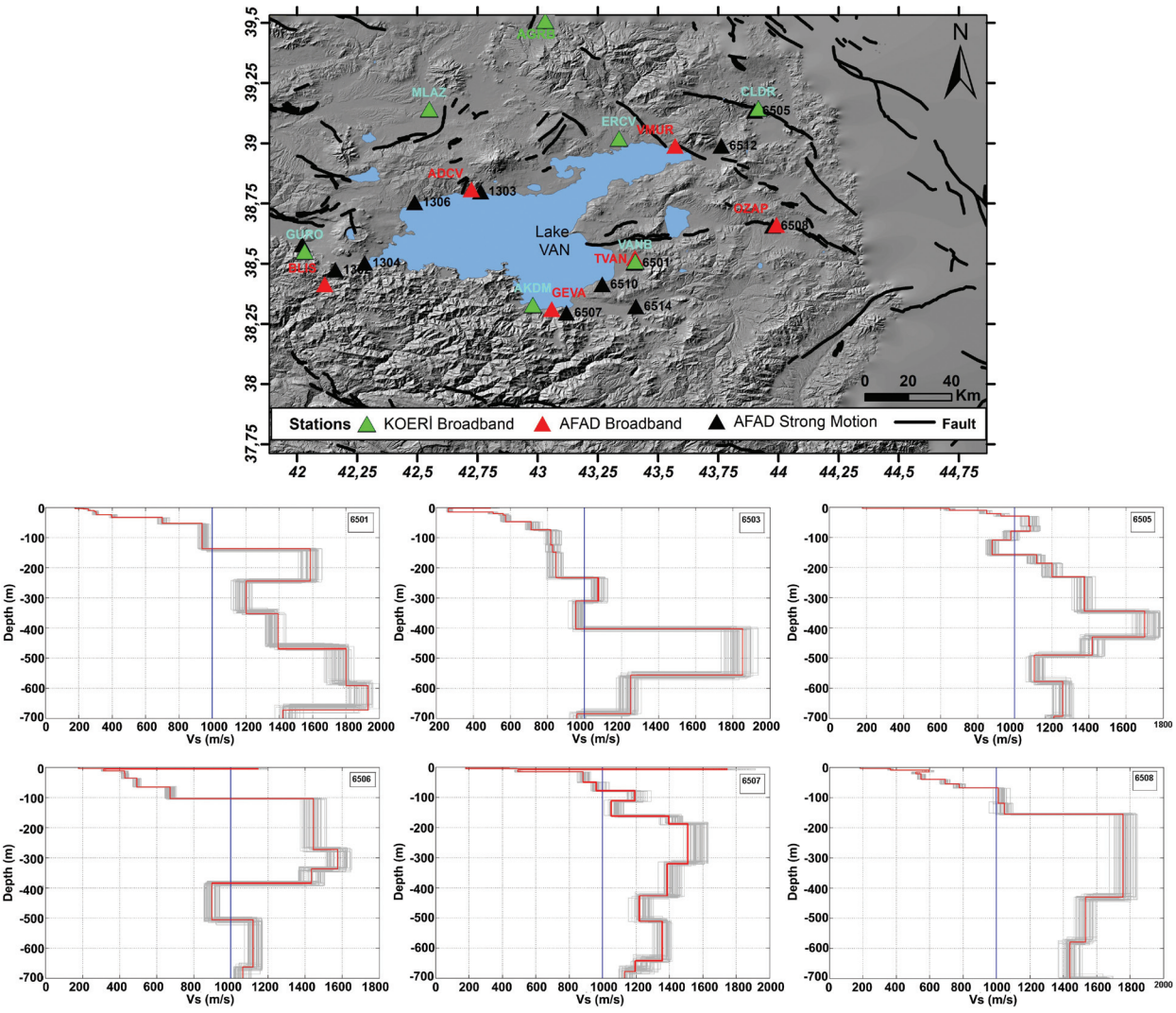

Fig. 5 The results of the optimum Vs velocity models for strong motion stations 6501, 6503, 6505, 6506, 6507, and 6508

studies (Fig. 6).

For stations ERCV, 6501 and 6508, which are located on the Quaternary aged water saturated and soft alluvium in the settlement areas of Van province and Erciş district, it was found that the Vs velocity values range from 180 to 580 m/s up to a depth of about 30 m. The Vs velocity results at all stations commonly increase with the depth. Sandy, silty and clay type of alluvial deposits are present from the surface to a depth of 30 m in the borehole data from station 6501. The highest amplitudes variety is between 0.5 and 5 Hz in the result spectrum (Fig. 6). In the station 6508, sand, gravel, silty, and clayey type of alluvial units may appear at a depth of almost 30 m. The predominant amplitude values are 1–5 Hz in the result spectrum (Fig. 6). In the borehole log of station ERCV (located in the district of Erciş), there are silty sand, sand, clay, and gravel types of units to a depth of about 30 m. The peak amplitude values vary from 0.5 to 2 Hz in the station spectrum (Fig. 6). The station 6505 is located in the district of Çaldıran. At this station, the Vs velocity ranges from 250 to 800 m/s. There is a comparatively high Vs velocity layer at about 10 m depth at this station. The Basalt type volcanic forms in the solid rock feature are found after soft and weak alluvial layers. The peak amplitudes range from 4–10 Hz in the curve (Fig. 6). At station 6510, silty, clayey, and travertine type of units may appear at a depth of almost 20 m. The predominant amplitude changes are 0.5–1 Hz in the spectrum (Fig. 6).

By using the Vs velocity sections obtained from EHVSR inversion, depth versus velocity sections in three different directions (A–A', B–B', and C–C') are created for the east of Lake Van (Figs 7 and S10–S11). These profiles were chosen due to the intense seismicity and active tectonic units that produced large and destructive earthquakes. The 2-D cross-sections of thicknesses and Vs velocities of the main seismic layers were created. The inversion results in topographic sections were correlated with stratigraphic boundaries and laterally interpolated. Accordingly, the subsurface profiles in the region were classified as low-velocity zone (< 400 m/s), high-velocity bedrock (≥ 760 m/s), and seismological bedrock (≥ 1500 m/s) (Figs 7 and S10–S11).

DISCUSSION

The A–A′ cross-section continues southwest to northeast along the east of the Lake Van region (Fig. 7). This cross-section covers a region of about 100 km. The depth-Vs velocity information of the strong ground motion and the broadband stations is

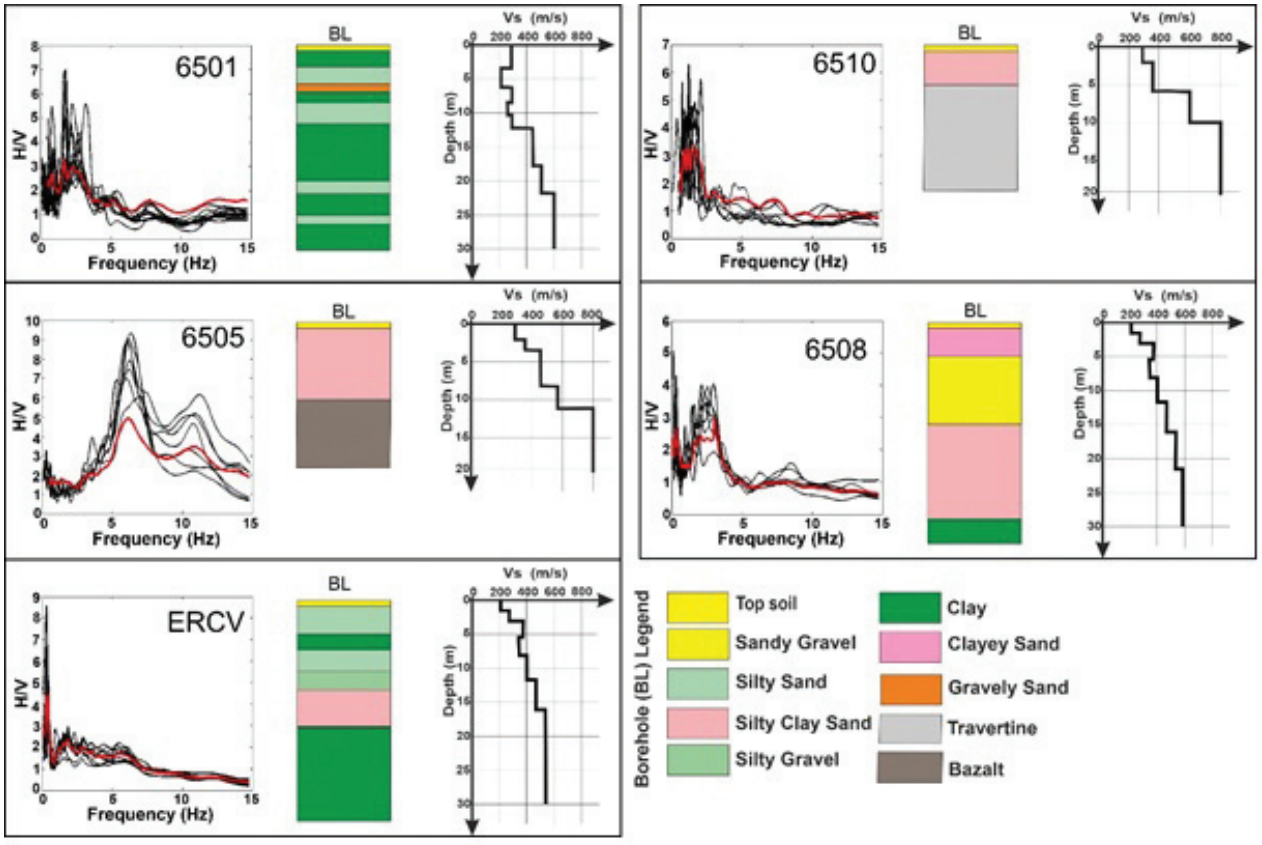

Fig. 6 Depth dependent Vs velocity cross-sections, borehole log and EHVSR results for the detailed stations 6501, 6505, 6508, 6510, and ERCV

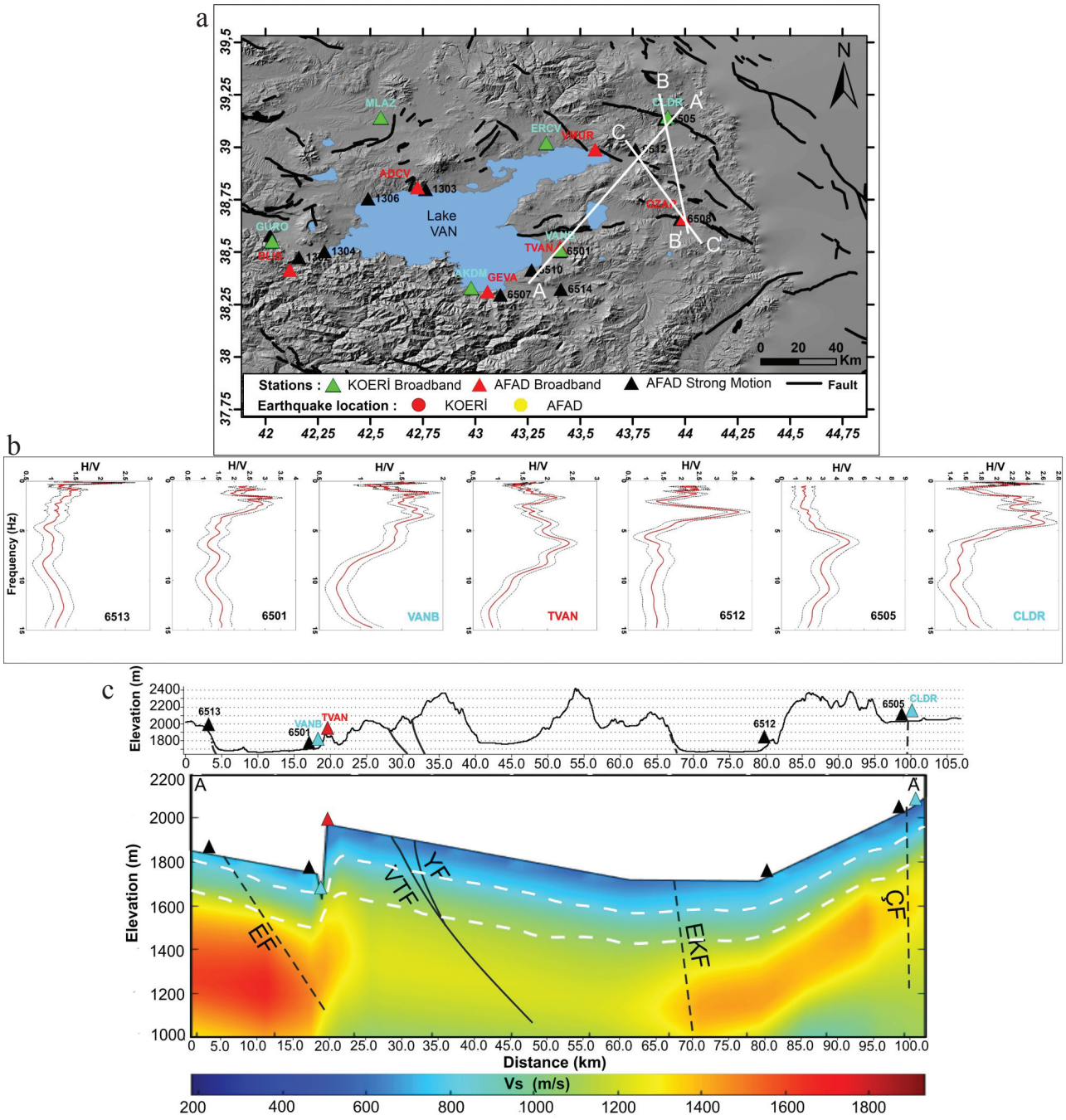

Fig. 7 (a) The map showing the direction of the cross-sections and the locations of earthquake stations. (**b**) The EHVSR curves are obtained from the inversion. (**c**) The southwest-northeast directional cross-section (A-A') is obtained from substation Vs velocities by inversion of the EHVSR curves. Abbreviations: VTF: Van Thrust Fault, EF: Edremit Fault, EKF: Erciş-Kocapınar Fault, YF: Yeniköşk Fault, ÇF: Çaldıran Fault Zone. Active faults in the region are shown by black lines (Emre *et al*. 2018)

shown in Fig. 7. The A–A' depth section is formed in the direction of intersecting the Van thrust fault, Erciş-Kocapınar fault, and Çaldıran fault zone, which previously caused destructive earthquakes in the region. The low-velocity zone (< 400 m/s), underlying bedrock (≥ 760 m/s), and seismological bedrock (≥ 1500 m/s) can be seen in the 2D depth versus Vs velocity cross-section plotted by using velocity models beneath the stations. Low-velocity layers exhibit different depths intervals throughout the cross-section. The shallow sediment units (< 20 m) are dominant in some regions; it also is observed to sediment thickness of 150–250 m or more from place to place. This low-velocity zone, which is thickly bedded from place to place, is a significant factor, especially in the eastern site of Lake Van, where the settlement areas are formed from the old lake and fluvial sediments. Because, in possible destructive earthquakes, these

low-velocity layers may affect the structural elements as factors that increase the earthquake effects. Low-velocity layers and bedrock depth structures with different depth intervals are extremely important in terms of the engineering seismological properties of geological units (elasticity, strength, stiffness, liquefaction, soil amplification, acceleration, etc.), seismicity, and the effects of earthquakes, as well as the geological characteristics of the environment. The EHVSR curves also confirm the frequency-bedrock depth relationship.

The B–B′ and C–C' cross-sections are formed in the northwest-southeast direction of intersecting the Çaldıran fault zone, Erciş-Kocapınar fault, and Özalp fault (Figs S10 and S11). In the B–B′ profile, the thickness of the sediment showed more lateral variations, ranging from 20 m to about 150 m. The deepest parts of sediment units were located at the end of the southeast site of the cross-section. In this cross-section, the Çaldıran fault zone and Özalp fault can be marked clearly (Fig. S10). In the C–C′ profile (Fig. S11), thinner sediment units are located in all components of the cross-section. As can be clearly seen in this profile, the high-velocity layers are observed in shallow depths, whilst relatively thinned sediments are viewed at around 10 m depth. The distribution of the Vs velocity is consistent with the topography of two cross-sections and is associated with the predominant frequency of the EHVSR. On the other hand, the EHVSR peaks correspond to sedimentary units.

CONCLUSIONS

The bedrock depth, one of the most critical parameters in determining engineering seismology investigation and soil-structure interaction studies, can be predicted with high accuracy using the EHVSR method. The depth to bedrock and the location of soil layers may be different behaviour and effect of seismic waves near the surface. In this study, twenty-two earthquakes around the Lake Van basin, recorded by twenty-nine (15 strong ground motion and 14 broadband) stations located in different geological units, are processed using the EHVSR inversion method. The geological structure and bedrock depth beneath the stations are determined from the obtained shear wave models.

As a result of the EHVSR analyses carried out in the study region, relatively low frequency values are defined due to the thickness of alluvial type formations under the earthquake stations, and also the frequency values increase to the different rock units under some earthquake stations. At some stations (6505, 6507, 6510, 1302, 1303, VANB, AGRB, TVAN, OZAP, and BLIS) more than one amplification peak is observed. It has been evaluated that obtaining multiple peaks may be depending on soil structures with more than one strong impedance variation. In general, these stations are located on weak and low-strength alluvial units. Furthermore, there are sub-alluvial rock units at various depth levels at some stations in the study area. The peak value in the EHVSR result spectra is generally chosen as the predominant frequency at these stations. In the study sites with weak soil units and deep alluvium, the amplitudes of the earthquake waves tend to increase, which can lead to high levels of damage in the near-surface soil.

In general, relatively high predominant period and amplification values were calculated due to the water-saturated, thick and weak alluvial units thickness under the earthquake stations in the region. In some regions, the period values decreased depending on the various rock units under the stations. These significant results indicated that the predominant period value is inversely proportional to the stability of the local geological structures and can be used for damage estimation after possible earthquakes.

By using the substation Vs velocity models obtained from the EHVSR inversion results, the velocity cross-sections of depth variations in three different directions are created in the east of Lake Van. The low-velocity zone (< 400 m/s), underlying bedrock (≥ 760 m/s), and seismological bedrock (≥ 1500 m/s) were seen in all three cross-sections. Low-velocity layers exhibit different depth intervals throughout the cross-sections. Depending on the Vs velocity variations obtained in the cross-sections, some important fault mechanisms that previously caused large and destructive earthquakes in the region (Van Thrust fault, Erciş-Kocapınar fault, Çaldıran fault, and Özalp fault) can be detected as visible. On the other hand, the EHVSR inversion results demonstrate that the low predominant frequencies reflect a lower Vs structure and deeper sediment distribution, while the high predominant frequencies represent a high Vs structure and thinner sediment distribution. The average bedrock depth changes from 10 and 250 m in the earthquake stations. The deepest bedrock depth is observed beneath stations 6501, 6506, 6507, 6508, 6514, VANB, ERCV, and OZAP.

The EHVSR inversion results can be helpful both for the determination of site amplification effects and for the geometry of seismic bedrock and coverage deposits. In other respect, if the shear wave inversion results are supported by geology and tectonic information, the obtained final models can be contributed to the subsurface velocity models achieved from geophysical methods. Consequently, a significant part of the Lake Van region may be seriously affected by earthquake strong ground motions. The planning of future structures can be based on the amplification value, predomi-

nant period, and bedrock depth maps of the area.

ACKNOWLEDGMENTS

The strong ground motion records are provided from the web page of the AFAD (https://tadas.afad.gov.tr). Broadband earthquake records are provided from the web page of the EIDA (http://orfeus-eu.org/webdc3/). The active fault database was taken from Emre *et al*. (2018). The open-source Geopsy software (www.geopsy.org) packages (GEOPSY 1997), prepared by the recommendations of the SESAME (2004) project, were used in the data processing. The authors thank the anonymous reviewers for their helpful comments that improved the quality of the manuscript.

Author Contribution

İA contributed to supervision; **İA** and **HA** contributed to methodology, software, data curation, formal analysis, and resources; **İA** and **HA** contributed to investigation, writing-original draft, writing-review & editing.

REFERENCES

Aki, K., Richards, P.G. 2002. *Quantitative Seismology*, 2nd Ed. In: University Science Books 68(5).

Akkaya, İ. 2015. The Application of HVSR Microtremor Survey Method in Yüksekova (Hakkari) Region, Eastern Turkey. *Journal of African Earth Sciences 109*, 87–95. https://doi.org/10.1016/j.jafrearsci.2015.05.018

Akkaya, İ. 2020a. Availability of seismic vulnerability index (Kg) in the assessment of building damage in Van, Eastern Turkey. *Earthquake Engineering and Engineering Vibration 19(1)*, 189–204. https://doi.org/10.1007/s11803-020-0556-z

Akkaya, İ. 2020b. Jeofizik Verilerinden Elde Edilen Sismik Zayıflık İndisinin Yapı Hasar Dağılımının Belirlenmesinde Kullanılabilirliği. *Bitlis Eren Üniversitesi Fen Bilimleri Dergisi 9(4)*, 1711–1723 [In Turkish].

Akkaya, İ. 2023. Investigation of site effect of Lake Van region (eastern Turkey) by using strong ground motion records. *Journal of Applied Geophysics 208(104867)*, 1–14.

Akkaya, İ., Özvan, A. 2019. Site characterization in the Van settlement (Eastern Turkey) using surface waves and HVSR microtremor methods. *Journal of Applied Geophysics 160*, 157–170. https://doi.org/10.1016/j.jappgeo.2018.11.009

Akkaya, İ., Özvan, A., Tapan, M., Şengül, M.A. 2015. Determining the site effects of 23 October 2011 earthquake (Van province, Turkey) on the rural areas using HVSR microtremor method. *Journal of Earth System Science 124(7)*, 1429–1443. https://doi.org/10.1007/s12040-015-0626-1

Akkaya, İ., Özvan, A., Akın, M., Akın, M.K., Övün, U. 2018. Comparison of SPT and Vs-Based Liquefaction Analyses: A Case Study in Erciş (Van, Turkey). *Acta Geophysica 66*, 21–38. https://doi.org/10.1007/s11600-017-0103-0

Alkan, A., Akkaya, İ. 2023 Investigation of site properties of the Çaldıran (Van, Eastern Turkey) settlement area using surface wave and microtremor methods. *Journal of African Earth Sciences 197*, 104737.

Alkan, H., Çınar, H., Oreshin, S. 2020. Lake Van (Southeastern Turkey) Experiment: Receiver Function Analyses of Lithospheric Structure from Teleseismic Observations. *Pure and Applied Geophysics 177*, 3891–3909.

Alkan, H., Büyüksaraç, A., Bektaş, Ö., Işık, E. 2021. Coulomb stress change before and after 24. 01. 2020 Sivrice (Elazığ) Earthquake (Mw = 6.8) on the East Anatolian Fault Zone. *Arabian Journal of Geosciences14*, 2648.

Alkan, H., Öztürk, S., Akkaya, İ. 2023. Seismic Hazard Implications in and Around the Yedisu Seismic Gap (Eastern Türkiye) Based on Coulomb Stress Changes, b-Values, and S-wave Velocity. *Pure and Applied Geophysics 180 (9)*, 3227–3248.

Aydın, U., Pamuk, E., Ozer, C. 2022. Investigation of soil dynamic characteristics at seismic stations using H/V spectral ratio method in Marmara Region, Turkey. *Natural Hazards 110*, 587–606. https://doi.org/10.1007/s11069-021-04959-4

Bard, P.Y. 1998. Microtremor Measurements: A tool for site effect estimation. *Proceedings of 2nd International Symposium on the Effect of Surface Geology on Seismic Motion 1–3 Dec Yokohama Japan 3*, 1251–1279.

Bignardi, S., Mantovani, A., Abu Zeid, N. 2016. Open HVSR: imaging the subsurface 2D/3D elastic properties through multiple HVSR modelling and inversion. *Computers and Geosciences 93*,103–113.

Bignardi, S., Yezzi, A.J., Fiussello, S., Comelli, A. 2018. Open HVSR-Processing toolkit: Enhanced HVSR processing of distributed microtremor measurements and spatial variation of their informative content. *Computers and Geosciences 120*, 10–20.

Büyüksaraç, A., Karaca, Ö., Eyisüren, O., Bektaş, Ö., Işık, E. 2022. Importance of Bedrock Depth Knowledge in Basins: Çanakkale (Dardanalles) Case History. In: Glavaš, H., Hadzima-Nyarko, M., Karakašić, M., Ademović, N., Avdaković, S. (eds), *30th International Conference on Organization and Technology of Maintenance (OTO 2021)*. Lecture Notes in Networks and Systems. *369*. Springer, Cham. https://doi.org/10.1007/978-3-030-92851-3_25

Büyüksaraç, A., Eyisüren, O., Bektaş, Ö., Karaca, Ö. 2023. Bedrock depth calculation of Çanakkale (Turkey) basin using Rayleigh ellipticity and microgravity survey. *Geophysica International 62*, 387–401.

Emre, O., Duman, T.Y., Ozalp, S., Saroglu, F., Olgun, S., Elmaci, H., Can, T. 2018. Active fault database of Turkey. *Bulletin of Earthquake Engineering 16*, 3229–3275.

Fah, D., Kind, F., Giardini, D. 2001. A theoreti-

cal investigation of average H/V ratios. *Geophysical Journal International 145*, 535–549. https://doi.org/10.1046/j.0956-540x.2001.01406.x

Gupta, R.K., Agrawal, M., Pal, S.K., Das, M.K. 2021. Seismic site characterization and site response study of Nirsa (India). *Natural Hazards 108*, 2033–2057. https://doi.org/10.1007/s11069-021-04767-w

Herak, M. 2008. ModelHVSR-A Matlab® tool to model horizontal-to-vertical spectral ratio of ambient noise. *Computers and Geosciences 34 (11)*, 1514–1526.

Ibs-von Seth, M., Wohlenberg, J. 1999. Microtremor measurements used to map thickness of soft sediments. *Bulletin of the Seismological Society of America 89*, 250–259.

Koçyiğit, A. 2013. New field and seismic data about the intraplate strike-slip deformation in Van region, East Anatolian plateau, Eastern Turkey. *Journal of Asian Earth Sciences 62*, 586–605. https://doi.org/10.1016/j.jseaes.2012.11.008

Koçyiğit, A., Yilmaz, A., Adamia, S., Kulashvili, S. 2001. Neotectonics of East Anatolian Plateau (Turkey) and Lesser Caucasus: Implication for transition from thrusting to strike-slip faulting. *Geodinamica Acta 14*, 177–195. https://doi.org/10.1080/09853111.2001.11432443

Lachet, C., Bard, P.Y. 1994. Numerical and Theoretical Investigations on the Possibilities and Limitations of Nakamura's Technique. *Journal of Physics Earth 42*, 377–397.

Lachet, C., Hatzfeld, D., Bard, P.Y., Theodulidis, N., Papaioannou, C., Savvaidis, A. 1996. Site effects and microzonation in the city of Thessaloniki (Greece): comparison of different approaches. *Bulletin of the Seismological Society of America 86*, 1692–1703.

Langston, C. 1977. Corvallis Oregon crustal and upper mantle receiver structure from teleseismic P and S waves. *Bulletin of the Seismological Society of America 67*, 713–724.

Lermo, J., Chavez-Garcia, F.J. 1993. Site effect evaluation using spectral ratios with only one station. *Bulletin of the Seismological Society of America* 83, 1574–1594.

Lermo, J., Chavez-Garcia, F.J. 1994. Are microtremors useful in site response evaluation?. *Bulletin of the Seismological Society of America 84*, 1350–1364.

Nakamura, Y. 1989. A method for dynamic characteristics estimation of subsurface using microtremor on the ground surface. *Railw Tech Res Inst Q Report 30*, 25–33.

Nakamura, Y. 2000. Clear Identification of Fundamental Idea of Nakamura's technique and its applications. *Proceedings of the 12th World Conference on Earthquake Engineering (WCEE), Auckland, New Zealand 30 January 4 February Paper No 2656*. http://www.nicee.org/wcee/

Nakamura, Y. 2008. On the H/V Spectrum. *The 14th World Conference on Earthquake Engineering, Beijing*. China. http://www.nicee.org/wcee/

Özer, Ç., Öztürk, S., Pamuk, E. 2022. Tectonic and structural characteristics of Erzurum and its surroundings (Eastern Turkey): a detailed comparison between different geophysical parameters. *Turkish Journal of Earth Sciences 31(1)*, 85–108. https://doi.org/10.3906/yer-2106-18

Özvan, A., Akkaya, İ., Tapan, M., Şengül, M.A. 2005. Van yerleş kesinin depremteh likesiveolası birde preminsonuç ları. *Deprem Sempozyumu Kocaeli* 23–25 Mart 2005 Kocaeli. [In Turkish].

Pamuk, E. 2019. Investigation of the local site effects in the northern part of the eastern Anatolian region, Turkey. *Bollettino di GeofisicaTeorica ed Applicata 60 (4)*, 549–568.

Pamuk, E., Ozer, C. 2020. The Site Effect Investigation with Using Horizontal-to-Vertical Spectral Ratio Method on Earthquake Data, South of Turkey. *Geotectonics 54(4)*, 563–576.

Parolai, S., Bormann, P., Milkereit, C. 2002. New relationships between Vs, thickness of sediments, and resonance frequency calculated by the H/V ratio of seismic noise for the Cologne area (Germany). *Bulletin of the Seismological Society of America 92*, 2521–2527.

Şaroğlu, F., Yılmaz, Y. 1986. Doğu Anadolu'daNeotektonik DönemdekiJeolojik Evrim veHavzaModelleri. *MTA Genel Müdürlüğü*, *Jeoloji Etütleri Dairesi Ankara* [In Turkish].

Sánchez-Sesma, F.J., Rodríguez, M., Iturrarán-Viveros, U., Luzón, F., Campillo, M. et al. 2011. A theory for microtremor H/V spectral ratio: Application for a layered medium. *Geophysical Journal International 186(1)*, 221–225.

Şengör, A.M.C., Kidd, W.S.F. 1979. Post-Collisional Tectonics of the Turkish–Iranian Plateau and a Comparison with Tibet. *Tectonophysics* 55, 361–376. https://doi.org/10.1016/0040-1951(79)90184-7

Sengul, M.A., Gürboğa, Ş., Akkaya, İ., Özvan, A. 2019. Deformation patterns in the Van region (Eastern Turkey) and their significance for the tectonic framework. *Geologica Carpathica 70*,193–208.

Tan, O., Tapırdamaz, M.C., Yörük, A. 2008. The Earthquakes Catalogues for Turkey. *Turkish Journal of Earth Science17*, 405–418.

Toker, M., Şengör, A., Demirel-Schlueter, F., Demirbağ, E., Çukur, D., İmren, C., et al. 2017a. The structural elements and tectonics of the Lake Van basin (Eastern Anatolia) from multi-channel seismic reflection profiles. *Journal of African Earth Sciences 129*, 165–178.

Toker, M., Pınar, A., Tur, H., 2017b. Source mechanisms and faulting analysis of the aftershocks in the Lake Erçek area (Eastern Anatolia, Turkey) during the 2011 Van event (Mw 7.1): Implications for the regional stress field and ongoing deformation processes. *Journal of Asian Earth Sciences150*, 73–86.

Tün, M., Pekkan, E., Özel, O., Güney, Y. 2016. An investigation into the bedrock depth in the Eskisehir Quaternary Basin (Turkey) using the microtremor method. *Geophysical Journal International 207,* 589–607. https://doi.org/10.1093/gji/ggw294

Utkucu, M. 2013. 23 October 2011 Van, Eastern Anatolia, Earthquake (Mw 7.1) and Seismotectonics of Lake Van

area. *Journal of Seismology 17,* 783–805.

Internet sources:

AFAD 2022. The Disaster and Emergency Management Authority of Turkey. Available: https://tadas.afad.gov.tr

GEOPSY 1997. Geophysical signal database for noise array processing. www.geopsy.org Accessed June 2021

KOERI 2021. Kandilli Observatory and Earthquake Research Institute. Available: https://tadas.afad.gov.tr

SESAME 2004. Guidelines for the implementation of the H/V spectral ratio technique on ambient vibrations: measurements, processing and interpretation SESAME European Research Project P12-Deliverable. D23.12 ftp://ftp.geo.uib.no/pub/seismo/Software/Sesame/Userguidelines/Sesame-HV-UserGuide lines.doc

Supporting Online Material